Thermal transport property of Ge_{34} and d-Ge investigated by molecular dynamics and the Slack's equation*

Wang Han-Fu(王汉夫)†, Chu Wei-Guo(褚卫国)‡, Guo Yan-Jun(郭延军), and Jin Hao(金 灏)§

National Center for Nanoscience and Technology of China, Beijing 100190, *China*

(Received 22 October 2009; revised manuscript received 25 December 2009)

In this study, we evaluate the values of lattice thermal conductivity $\kappa_{\rm L}$ of type II Ge clathrate (Ge_{34}) and diamond phase Ge crystal (d-Ge) with the equilibrium molecular dynamics (EMD) method and the Slack's equation. The key parameters of the Slack's equation are derived from the thermodynamic properties obtained from the lattice dynamics (LD) calculations. The empirical Tersoff's potential is used in both EMD and LD simulations. The thermal conductivities of d-Ge calculated by both methods are in accordance with the experimental values. The predictions of the Slack's equation are consistent with the EMD results above 250 K for both Ge_{34} and d-Ge. In a temperature range of 200–1000 K, the $\kappa_{\rm L}$ value of d-Ge is about several times larger than that of Ge_{34}.

Keywords: clathrate, thermal conductivity, molecular dynamics simulation, the Slack's equation
PACC: 6500, 6670, 7115Q, 6320

1. Introduction

Clathrate frameworks formed by Si and Ge elements have attracted considerable attention in recent years due to their interesting high pressure behaviours[1] and potential applications in thermoelectrics[2−4] and superconductivity.[5,6] In Si and Ge clathrates, the basic building blocks are covalently bonded $Si_{20}(Ge_{20})$, $Si_{24}(Ge_{24})$ or $Si_{28}(Ge_{28})$ polyhedral cages. They are so arranged that they share common pentagonal and hexagonal faces. Impurity atoms incorporated into the cages during synthesis are believed to introduce 'rattling' vibrational modes to reduce the lattice thermal conductivity $\kappa_{\rm L}$ without significantly affecting the electrical conductivity of the materials. This idea, termed 'phonon glass and electron crystal' (PGEC), is proposed as a unique way to enhance the figure of merit ZT of thermoelectrics.[7] In fact, the atomic 'rattler' may be not the only factor that causes the low $\kappa_{\rm L}$ of the clathrates. As suggested by Dong *et al.*,[8] the complex structure of the guest-free clathrate itself could lead to a thermal conductivity lower than that of diamond phase (d-Ge).

Experimentally, the thermal conductivity of guest-free Si_{34} (type-II clathrate) was found to be close to that of amorphous SiO_2.[9] Though the value was obtained on a polycrystalline Si_{34} sample, it should be correlated to the intrinsic low thermal transport ability of single crystal Si_{34}.

Actually, it is of fundamental research interest to obtain the thermal conductivities of the single crystal clathrates experimentally or theoretically. Lack of experimental thermal conductivity data on single crystals may be attributed to the difficulties in preparing samples. Under such a circumstance, theoretical methods like molecular dynamics (MD) method become valuable tools to estimate the intrinsic lattice thermal conductivity. To apply the MD method, one does not need know in advance the detailed phonon scattering mechanisms involved in the system. A reliable empirical potential is the most important prerequisite to perform the simulation.[8,10−19]

Besides the MD approach, the $\kappa_{\rm L}$ of the solids can also be evaluated based on analytical methods such as Callaway model[20] and Holland model.[21] They provide deep insight into the detailed phonon scattering processes on the basis of many approximations and assumptions. In contrast to these complicated models, the Slack's equation[22] offers a relatively simple way to estimate the $\kappa_{\rm L}$ of a perfect bulk crystal in a

*Project supported by the Knowledge Innovation Program of the Chinese Academy of Sciences (Grant No. KJCX2-YW-H20).
†E-mail: wanghf@nanoctr.cn
‡E-mail: wgchu@nanoctr.cn
§E-mail: hjin@nanoctr.cn
© 2010 Chinese Physical Society and IOP Publishing Ltd

temperature range where the Umklapp process dominates. The equation can be written as

$$\kappa_{\rm L} = A\overline{M}\theta_{\rm a}^3\delta n^{1/3}/(\gamma^2 T), \quad T > \theta_{\rm a}, \tag{1}$$

where $\overline{M}$ (amu) is the average atomic mass, $\theta_{\rm a}$ (K) the acoustic Debye temperature, δ^3 (Å^3) (1 Å=0.1 nm) the average volume per atom, n the number of atoms in each primitive cell, γ the high temperature Grüneisen parameter, and $A = 2.43 \times 10^{-6}/(1 - 0.514/\gamma + 0.228/\gamma^2)$ for $\kappa_{\rm L}$ in W/m/K. In the Slack's equation, $\theta_{\rm a}$ and γ are two important parameters that significantly affect the magnitude of $\kappa_{\rm L}$. In principle, they can be derived not only from the experimental data, but also from the theoretical calculations.

The previous MD studies on the thermal transports of silicon and germanium clathrates are relatively rare. Dong *et al.* calculated the thermal conductivities of the Ge_{46}(type-I clathrate) and its guest-containing counterpart Sr_6Ge_{46} at room temperature by using the equilibrium molecular dynamics (EMD) in conjunction with the Tersoff's potential.[8] For pristine Ge_{46}, they found that the reduction of $\kappa_{\rm L}$ with respect to that of d-Ge could be explained by the scaling of $\kappa_{\rm L}$ with the number of atoms in the primitive cell. More recently, the thermal transport properties of Si_{34} and Si_{46} nanowires were investigated by Ponomareva *et al.* through using the non-equilibrium molecular dynamics (NEMD).[17]

In the present study, we estimate the lattice thermal conductivity $\kappa_{\rm L}$ of two types of Ge structures, namely Ge_{34} (type-II clathrate) and d-Ge, with the EMD method as well as the Slack's equation. Both crystals belong to cubic space group $Fd\bar{3}m$ (No. 227), while Ge_{34} has 34 atoms per primitive unit cell, and d-Ge has only 2 atoms per primitive cell. In the EMD simulation, the heat flux fluctuations are recorded to compute the thermal conductivity based on the Green–Kubo fluctuation–dissipation theorem. The value of $\kappa_{\rm L}$ is calculated as a function of temperature up to 1000 K.

To apply the Slack's equation, the phonon properties of Ge_{34} and d-Ge are first obtained based on the lattice dynamics (LD) calculations.[23−26] (Note that the empirical Tersoff's potential is employed in both LD and MD calculations.) We then evaluate temperature dependent thermodynamic properties including Helmholtz free energy, bulk modulus, thermal expansion coefficient, Debye temperature and overall Grüneisen parameter. The parameters $\theta_{\rm a}$ and γ of the Slack's equation can be derived from the above calculations. We compare the $\kappa_{\rm L}$ values obtained from the MD calculations with those from the Slack's equation for Ge_{34} and d-Ge. In addition, the calculated thermal conductivity of d-Ge is also compared with the experimental result.

2. Computational methods

In this study, the parameters of the empirical Tersoff's potential for Ge are cited from Ref. [27].

The LD calculations are carried out to evaluate structural and vibrational properties of Ge_{34} and d-Ge by using the General Utility Lattice Program (GULP) code.[28] We use a $2 \times 2 \times 2$ supercell containing 1088 atoms as a simulation box for Ge_{34}, and a 4×4×4 supercell containing 512 atoms for d-Ge. The structures of the two crystals are first optimized to acquire their equilibrium lattice constants at 0 K under a constant pressure of 0 GPa. The phonon dispersion curves and the phonon densities of states (PDOSs) are then calculated based on these equilibrium structures. To obtain PDOSs, a 10×10×10 k-grid mesh is used in Brillouin zone integration for Ge_{34}, and a 20×20×20 k-grid mesh for d-Ge.

In order to compute temperature dependent thermodynamic properties, static energy and phonon density of states are calculated at several cell volumes for both d-Ge and Ge_{34}. In the quasi-harmonic approximation, the temperature dependent Helmholtz free energy $F(V,T)$ in simulation cell volume V can be written as[23]

$$F(V,T) = E_{\rm s}(V) + \int_0^{\omega_{\rm MAX}} \Big(\hbar\omega/2 + k_{\rm B}T \times \ln\left[1 - \exp(-\hbar\omega/k_{\rm B}T)\right] \Big) \times D\left(V,\omega\right) {\rm d}\omega, \tag{2}$$

where $E_{\rm s}$ is the static energy at 0 K, $D(\omega, V)$ is the phonon density of states (PDOS) obtained from the LD calculations, V denotes the volume of the simulation cell, ω is the frequency, $\hbar$ is the Planck's constant, $k_{\rm B}$ represents the Boltzmann's constant. The second term in Eq. (2) represents the contributions to the Helmholtz free energy from the zero-point motion and thermal excitation of the phonons.

At a fixed temperature T, the values of $F(V,T)$ obtained in different volumes can be fitted to a third-order Birch–Murnaghan equation of state (EOS):[26]

$$F(V,T) = F_0(T) + \frac{9}{8}B(T)V_0(T)\left[\left(\frac{V_0(T)}{V(T)}\right)^{2/3} - 1\right]^2 \left\{1 + \left(\frac{4 - B(T)'}{2}\right)\left[1 - \left(\frac{V_0(T)}{V(T)}\right)^{2/3}\right]\right\}, \quad (3)$$

where B is the bulk modulus, and B' the pressure derivative of bulk modulus. We can obtain equilibrium Helmholtz free energy $F_{0.}(T)$, equilibrium volume $V_0(T)$ and bulk modulus $B(T)$ from the fitting procedure.

The MD program used in this study is modified from a Fortran code originally developed by Li *et al.*[10,29] All simulations are performed in cubic simulation cells with periodic boundary condition (PBC) applied. The simulations are carried out with a time step of 0.764 fs for a total of 8.6×10^6 steps in the case of Ge_{34}, and 1.7×10^7 steps in the case of d-Ge. The systems are allowed to relax to reach the equilibrium at the indicated temperature and zero external pressure for 1.4×10^5 time steps under the isobaric and isothermal ensemble (NPT) using a thermal bath and a constant pressure algorithm of Parrinello and Rahman.[30] The system is evolved by solving the Newtonian equations with the Gear-predictor–corrector algorithm.[31] The initial velocities of the atoms are assigned according to the Maxwellian distribution. After the equilibrium phase, the simulation proceeds in a microcanonical ensemble (NVE) in which the instantaneous heat current $\overrightarrow{J(t)}$[10] is expressed as

$$\overrightarrow{J(t)} = \sum_i \left((E_i - h)\,\overrightarrow{v_i} + \sum_{j\neq i} \overrightarrow{r_{ij}} \left(\frac{\partial E_i}{\partial \overrightarrow{r_j}}\,\overrightarrow{v}_j \right) \right), \quad (4)$$

where E_i is the internal energy of atom i, $\overrightarrow{v_i}$ the atomic velocity, and h the average enthalpy per atom. At the end of the MD run, heat current autocorrelation function (HCACF) $\langle \overrightarrow{J(t)} \cdot \overrightarrow{J(0)} \rangle$ is computed from $\overrightarrow{J(t)}$ by applying the fast Fourier-transform algorithm and the spectral techniques.[10,32]

The MD thermal conductivity $\kappa_{\rm MD}$ is derived from HCACF based on the Green–Kubo formula[10] to be

$$\kappa_{\rm MD} = \frac{1}{3k_{\rm B}T_{\rm MD}^2 V}\int_0^\infty \sum_{\alpha=x,y,z} \langle J_\alpha(t)\cdot J_\alpha(0)\rangle {\rm d}t, \quad (5)$$

where α denotes the three Cartesian coordinates, and V the volume. By defining $G(t) = \Big(\sum_{\alpha=x,y,z} \langle J_\alpha(t)\cdot J_\alpha(0)\rangle\Big)/3k_{\rm B}T_{\rm MD}^2 V$, Eq. (5) is rewritten as

$$\kappa_{\rm MD} = \int_0^\infty G(t){\rm d}t. \quad (6)$$

When the classic MD calculation is performed below the Debye temperature, a correction may be needed by taking into account the quantum effects such as zero-point vibration. The Debye temperature is estimated to be 372 K for d-Ge, and 324 K for Ge_{34}.[33] Since our calculation is to be extended to the case where temperature is as low as 200 K, it is appropriate to include a 'quantum effect' correction. To do this, a method proposed by Wang *et al.*[34] is adopted in which the temperature of the 'real' quantum system, $T_{\rm Real}$, is scaled to the temperature $T_{\rm MD}$ of the classical MD system by equating the mean kinetic energies of both systems. Temperature $T_{\rm MD}$ is expressed as

$$T_{\rm MD} = \frac{1}{k_{\rm B}}\int_0^{\omega_{\rm MAX}} \hbar\omega \left(\frac{1}{2} + \frac{1}{\exp(\hbar\omega/k_{\rm B}T_{\rm Real}) - 1}\right) D(\omega)\,{\rm d}\omega. \quad (7)$$

Finally, $\kappa_{\rm MD}$ is multiplied by a temperature gradient factor ${\rm d}T_{\rm MD}/{\rm d}T_{\rm Real}$[10] to obtain the thermal conductivity κ of the real system as follows:

$$\kappa = \kappa_{\rm MD}\frac{{\rm d}T_{\rm MD}}{{\rm d}T_{\rm Real}}. \quad (8)$$

To minimize the statistical errors, the final results of κ are averaged from the outputs of several independent MD runs with different initial configurations.

3. Results and discussion

3.1. Phonon properties

Table 1 lists the equilibrium structural, energetic and elastic properties of d-Ge and Ge_{34} which are calculated using the GULP code. They show good agreement with the values given in the relevant literature.[33,35,36]

Table 1. Static structural, energetic and elastic properties of Ge_{34} and d-Ge.

	Ge_{34}		d-Ge	
	GULP	literatures	GULP	Literatures
Lattice constant/Å	15.231	15.13[a]	5.65	5.64[a]
atomic volume/(Å^3/atom)	25.979	24.454[b]	22.587	21.361[b]
cohesive energy/(eV/atom)	3.816	3.81[b]	3.861	3.85[b]
bulk modulus/GPa	64.9	67[b]	76.1	79.0[b]
				75.0[c]
shear modulus/GPa	39.0	–	54.5	55.0[c]

[a]Ref. [35], *ab initio* method. [b]Ref. [36], *ab initio* method. [c]Ref. [33], computed from experimental elastic constants.

The phonon dispersion curves of Ge_{34} and d-Ge are plotted along several high-symmetry lines in the first Brillouin zone (FBZ) (Fig. 1). The PDOS spectra are displayed along side of the dispersion curves. The overall shapes of the phonon dispersion curves and the PDOS spectra of Ge_{34} or d-Ge are in accordance with the previous theoretical studies based on the first-principles calculations.[35,37] It has been shown that the Tersoff's potential is stiff for angular distortions, which leads to the overestimation of the frequencies of transverse acoustic (TA) modes at the zone boundary of d-Si.[38,39] The observation also holds true for d-Ge when it is treated with the Tersoff's potential. The calculated TA frequencies at L and X points in FBZ of d-Ge are 123.8 cm^{-1} and 177.3 cm^{-1}, respectively, which are about 100% larger than the experimental values (63 cm^{-1} and 80 cm^{-1}, respectively).[37]

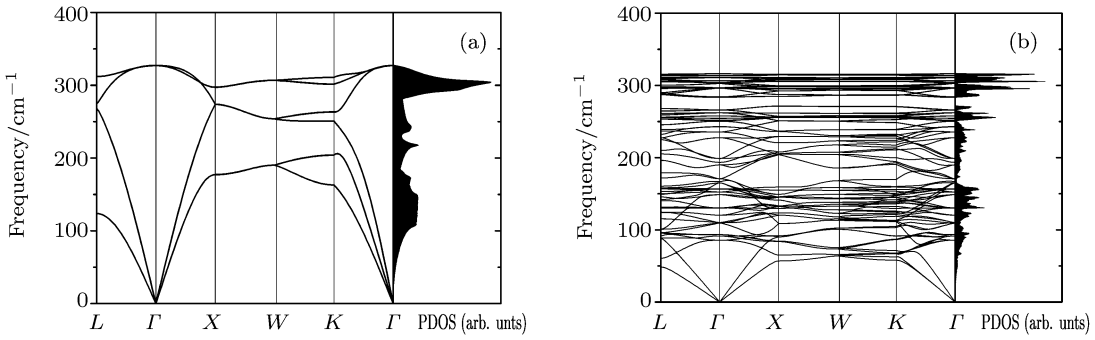


Fig. 1. Phonon dispersion curves along several high-symmetry lines in the first Brillouin zone of the primitive cell for d-Ge (a) and Ge_{34} (b). The spectra for phonon density of states are also plotted together for comparison.

In the case of Ge_{34}, the phonon modes below 60 cm^{-1} can be roughly assigned to the acoustic-like bands, while the optical-like bands are located approximately in a range from 60 to 327 cm^{-1}. The dispersion curves are relatively flat in the optical-like band region, which leads to sharp peaks in the PDOS spectra. (Fig. 1) Phonon gaps in PDOS can be found around 273–282 cm^{-1} for Ge_{34}. The gap is attributed to the fact that the clathrate framework has more than one type of bond length, which is equivalent to having more than one type of force constant in the network.[40] The overestimation of the TA frequencies at zone boundary can be also found in Ge_{34}. By digitizing Fig. 5(b) in Ref. [35], the TA frequencies calculated from the *ab initio* calculations are found to be around 30 cm^{-1} at L point, and 33 cm^{-1} at X point. They are roughly 60% of the calculated values in this work (48 cm^{-1} at L point and 57 cm^{-1} at X point).

3.2. Equation of state

Figure 2 shows the Helmholtz free energies of Ge_{34} and d-Ge versus average atomic volume at five different temperatures. At a given temperature T, the $F(V,T)$ values obtained at different volumes are fitted to the Birch-Murnaghan equation of state. The fitting results are plotted in the figure as dash lines. The minimum of each curve is corresponding to $F_0(T)$, the equilibrium Helmholtz free energy at a given temperature T.

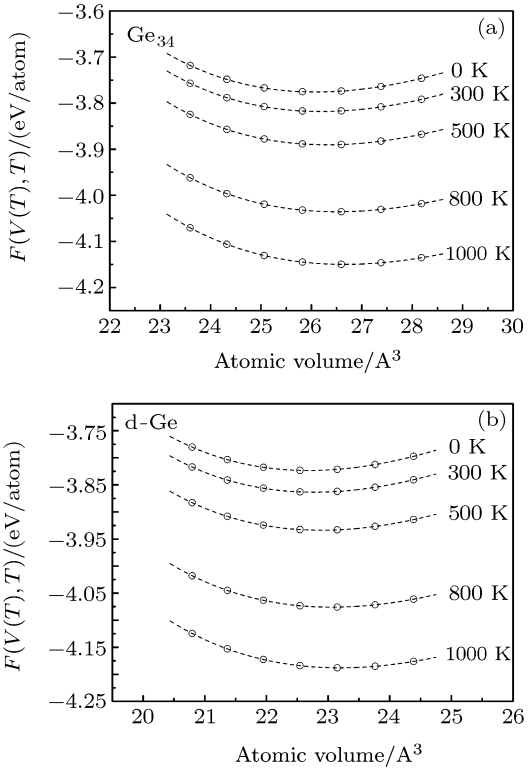


Fig. 2. Helmholtz free energies of Ge_{34}(a) and d-Ge (b) versus average atomic volume at several temperatures. The empty circles denote the data evaluated from Eq. (2); the dash lines represent the fit to the Birch–Murnaghan equation of state.

The curves for $F_0(T)$ versus temperature for Ge_{34} and d-Ge are presented in Fig. 3. It can be seen that $F_0(T)$ of d-Ge is more negative than that of Ge_{34} in the whole temperature range.

The values of equilibrium lattice constant $a_0(T)$ of two crystals are displayed in Fig. 4(a) and Fig. 4(b), respectively. At 0 K, the lattice constant is 15.25 Å for Ge_{34}, and 5.66 Å for d-Ge. The results are consistent with those obtained directly from the optimization procedure through using the GULP code (see Table 1).

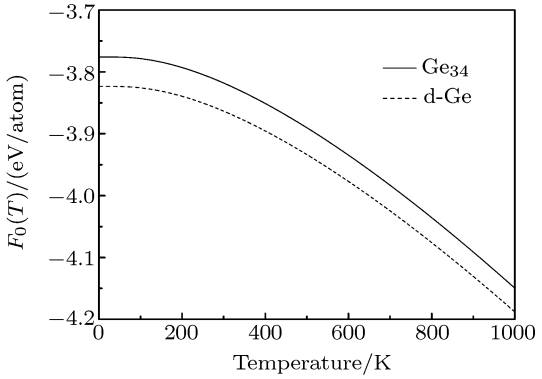


Fig. 3. Equilibrium Helmholtz free energies of Ge_{34} (solid line) and d-Ge (dashed line) versus temperature.

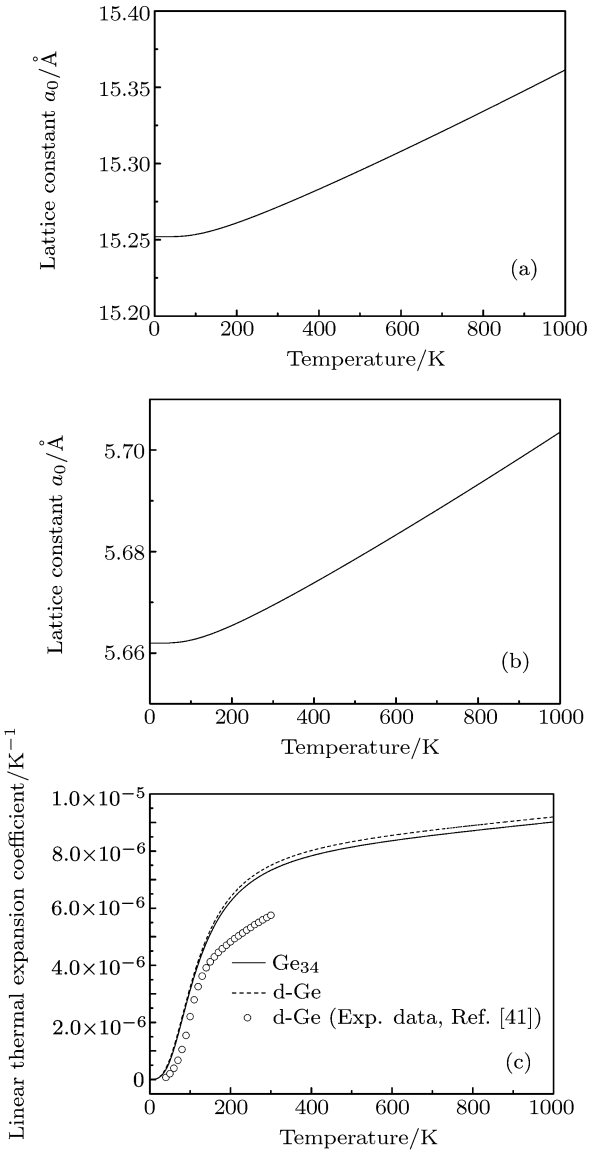


Fig. 4. Lattice constants of Ge_{34} (a), d-Ge (b) and their linear thermal expansion coefficients (c) versus temperature. Experimental thermal expansion coefficients of d-Ge are also presented for comparison.

The linear thermal expansion coefficient $\alpha_{\rm L}$ is given as

$$\alpha_{\rm L}(T) = \frac{1}{a(T)}\frac{{\rm d}a(T)}{{\rm d}T}. \quad (9)$$

Figure 4(c) illustrates the variations of the calculated values of $\alpha_{\rm L}$ of Ge_{34} and d-Ge with temperature. Between 0 K and 1000 K, the calculated thermal expansion coefficient of Ge_{34} is very close to that of d-Ge. On the other hand, the experimental values[41] of d-Ge, which are plotted in the same figure, are significantly smaller than the calculated results. Porter *et al.* showed that the Tersoff's potential behaved poorly on calculating $\alpha_{\rm L}$ of d-Si due to the unrealistic volume dependence of TA modes.[38] Therefore, the same reason should be responsible for the less satisfactory calculations on $\alpha_{\rm L}$ of d-Ge in this work.

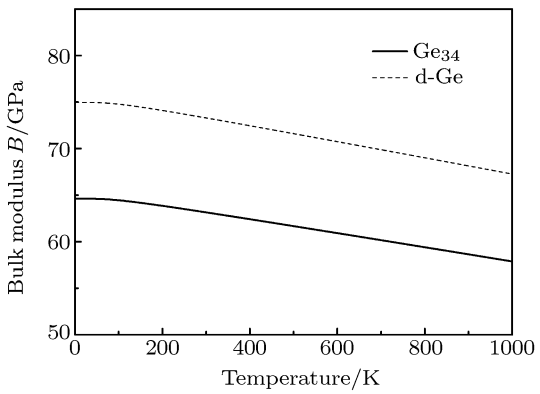


Fig. 5. Bulk moduli of Ge_{34} and d-Ge versus temperature.

The bulk moduli of both crystals are found to decrease with temperature increasing (Fig. 5). At 0 K, B is 75.0 GPa for d-Ge, and 64.6 GPa for Ge_{34}, which confirms the results calculated directly from the GULP code. (see Table 1)

3.3. Specific heat and Debye temperature

From the phonon density of states of the optimized structure, the values of specific heat at constant volume $C_{\rm V}$ can be computed for Ge_{34} and d-Ge in the harmonic approximation from

$$C_{\rm V}(T) = 3k_{\rm B}\int_0^{\omega_{\rm MAX}}\left(\frac{\hbar\omega}{k_{\rm B}T}\right)^2 \times\frac{\exp(\hbar\omega/k_{\rm B}T)}{[\exp(\hbar\omega/k_{\rm B}T)-1]^2}D(\omega)\,{\rm d}\omega. \quad (10)$$

As shown in Fig. 6(a), the $C_{\rm V}$ curves of two crystals almost overlap with each other, and they approach to the classical Dulong–Petit limit ($C_{\rm V} = 3k_B$/atom) at higher temperatures. The experimental specific heat[42] of d-Ge is slightly larger than the calculated value below 300 K.

In the classic Debye model, the heat capacity at constant volume $C_V^{\rm D}$ is written as[43]

$$C_{\rm V}^{\rm D}(T) = 9k_{\rm B}\left(\frac{T}{\Theta_{\rm D}(T)}\right)^3\int_0^{\frac{\Theta_{\rm D}}{T}}\frac{x^4{\rm e}^x}{({\rm e}^x-1)^2}{\rm d}x, \quad (11)$$

where $\Theta_{\rm D}(T)$ is the Debye temperature.

The $\Theta_{\rm D}(T)$ can be solved numerically by equating $C_{\rm V}(T)$ of Eq. (10) and $C_{\rm V}^{\rm D}(T)$ of Eq. (11). At a given temperature T, $\Theta_{\rm D}(T)$ is continuously varied as a parameter to calculate $C_{\rm V}^{\rm D}(T)$ until $C_{\rm V}^{\rm D}(T)$ equals $C_{\rm V}(T)$. The final value of $\Theta_{\rm D}(T)$ is the Debye temperature at temperature T. Figure 6(b) indicates that the Ge_{34} has a lower Debye temperature than the d-Ge in a temperature range of 0–1000 K. The Debye temperatures of Ge_{34} and d-Ge were previously calculated to be 324 K and 372 K, respectively, from the elastic constants that were obtained from the lattice dynamics calculations by using the Tersoff's potential.[33] They are actually corresponding to the calculated Debye temperatures at 0 K in the present work respectively (see Fig. 6(b)).

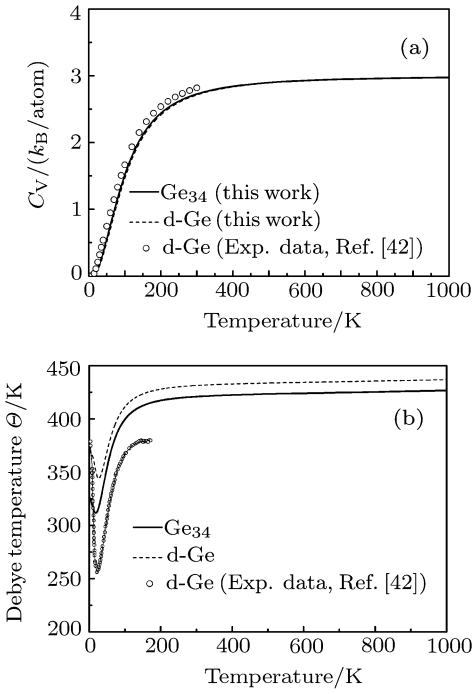


Fig. 6. Curves for constant volume specific heat (a) and Debye temperature (b) of Ge_{34} and d-Ge versus temperature. Experimental specific heat and Debye temperature of d-Ge are also displayed for comparison.

Above 0 K, the calculated Debye temperature of d-Ge is larger than the experimental value.[42] It should be noted that all $\Theta_{\rm D}(T)$ curves each show a curve minimum in the low temperature region. It will be used to determine the acoustic Debye temperature of the Slack's equation in Subsection 3.6.

3.4. Overall Grüneisen parameter

The Grüneisen parameter γ is used to account for the anharmonicity of the lattice vibration of the crystal. The overall Grüneisen parameter is determined from linear thermal expansion coefficient $\alpha_{\rm l}$, bulk modulus B, specific heat $C_{\rm V}$ and molar volume $V_{\rm m}(T)$ to be

$$\gamma(T) = 3\alpha_{\rm L}(T)B(T)V_{\rm m}(T)/C_{\rm V}(T). \qquad (12)$$

In Fig. 7, the calculated values of γ for Ge_{34} and d-Ge are displayed as solid line and dash line, respectively. Below 200 K, γ values of both crystals increase quickly with temperature. As temperature increases further, γ value stays almost constant. The γ value of d-Ge is slightly larger than that of Ge_{34} in the plateau region. Compared with the experiment result[41,44] and *ab initio* calculation,[45] the present result overestimates the Grüneisen parameter of d-Ge. As mentioned above, this should be attributed to the inadequacy of the Tersoff's potential for treating the volume dependence of TA modes.[38,39]

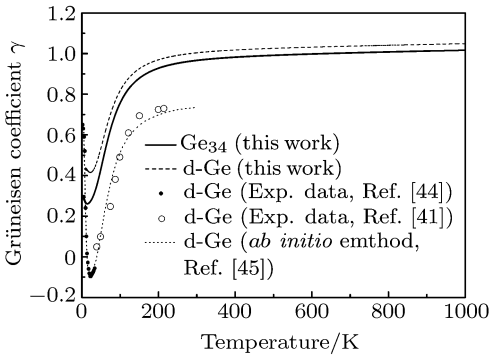


Fig. 7. Overall Grüneisen parameters of Ge_{34} and d-Ge against temperature. For d-Ge, experimental and *ab initio* values are displayed for comparison.

3.5. Molecular dynamics

3.5.1. Temperature scaling curve

In the MD simulations of this study, the quantum corrections of temperature have been applied to Ge_{34} and d-Ge. The temperature scaling relations between $T_{\rm MD}$ and real temperature $T_{\rm Real}$ are depicted in Fig.8. The temperature gradient factor $\mathrm{d}T_{\rm MD}/\mathrm{d}T_{\rm Real}$ is also plotted in the same figure.

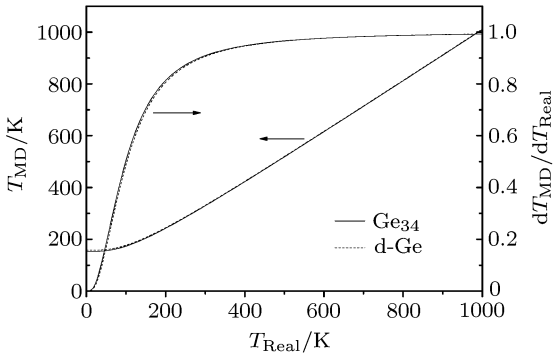


Fig. 8. Curves for $T_{\rm MD}$ and $\mathrm{d}T_{\rm MD}/\mathrm{d}T_{\rm Real}$ versus $T_{\rm Real}$ of Ge_{34} (solid line) and d-Ge (dashd line).

3.5.2. Normalized correlation function $g(t)$

Following the notation in Ref. [8], a normalized correlation function $g(t)$ can be defined as $g(t) = G(t)/G(0)$. By inserting $g(t)$ into Eq. (6), $\kappa_{\rm MD}$ is rewritten as

$$\kappa_{\rm MD} = G(0)\int_0^\infty g(t)\mathrm{d}t. \qquad (13)$$

Figure 9 shows the normalized correlation function $g(t)$ curves obtained at 400 K for d-Ge and Ge_{34}. The MD thermal conductivity is calculated by integrating $g(t)$ in Eq. (13). In order to perform integration, the $g(t)$ curve is first fitted with a double exponential decay function[12] within a time range [0, $t_{\rm F}$] ps and given as

$$g\,(t) = A_1\exp(-t/\tau_1) + A_2\exp(-t/\tau_2), \qquad (14)$$

where A and τ are the constants that need to be determined from the fitting procedure. In principle, the values of $t_{\rm F}$ are chosen based on the simulation temperature. At lower temperatures, a larger $t_{\rm F}$ should be used.

By inserting Eq. (14) into Eq. (13), we have

$$\kappa_{\rm MD} = G(0)(A_1\tau_1 + A_2\tau_2). \qquad (15)$$

With Eq. (8) and Eq. (15), the thermal conductivity κ at $T_{\rm Real}$ can be finally obtained.

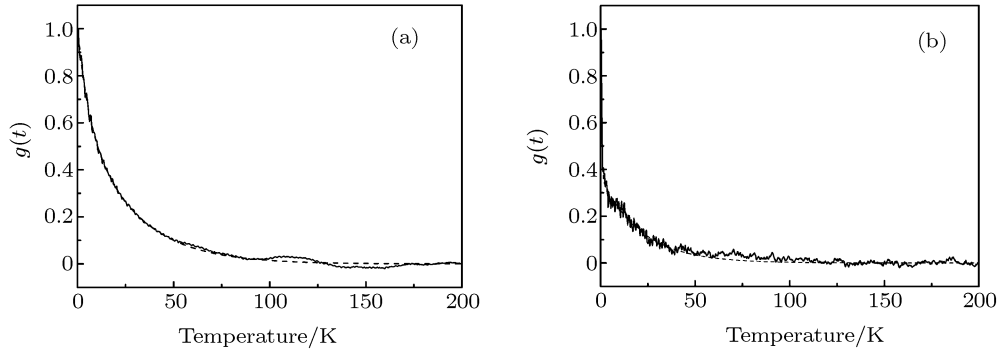


Fig. 9. Curves for normalized correlation function $g(t)$ (solid line) of d-Ge (a) and Ge_{34} (b) at $T_{\rm Real} = 400$ K and they are fitted by the double exponential decay curves (dash lines).

3.5.3. Finite size effect

It has been known that the finite size of the simulation box affects the value of the calculated thermal conductivity.[14,16] To evaluate the finite-size effect, we calculate the thermal conductivities of Ge_{34} and d-Ge with different simulation cell sizes at 300 K (Table 2). The convergences of the thermal conductivities are found to be reached at a cell size of 512 atoms for d-Ge, and 3672 atoms for Ge_{34} separately. In the following calculations, we use a simulation box containing 1728 atoms for d-Ge, and another containing 3672 atoms for Ge_{34}.

Table 2. Finite size effect of the simulation cell on thermal conductivities of d-Ge and Ge_{34} at 300 K.

crystal	number of atoms	κ/(W/K/m)
d-Ge	512	60.01 ± 4.52
	1000	62.20 ± 0.94
	1728	59.80 ± 7.94
Ge_{34}	1088	7.93 ±0.43
	3672	10.99±1.77
	8704	10.01 ±0.62

The previous studies have shown that the thermal conductivity can reach convergence even the size of the simulation box, L, is much smaller than the phonon mean free path λ. The value of λ can be estimated through the following expression:[46]

$$\kappa = C\overline{v}\lambda/3, \tag{16}$$

where C is the specific heat capacity per unit volume, and $\overline{v}$ is the average phonon velocity given by[47]

$$\overline{v} = \left[\frac{1}{3}\left(\frac{3\rho}{3B+4G}\right)^{3/2} + \frac{2}{3}\left(\frac{\rho}{G}\right)^{3/2}\right]^{-1/3}, \tag{17}$$

where B is the bulk modulus, G the shear modulus, and ρ the density. If the calculated thermal conductivities in Table 2 are used (60 W/m/K obtained from a 6×6×6 cell for d-Ge, 11 W/m/K from a 3×3×3 cell for Ge_{34}), the values of phonon mean free path at room temperature are found to be 307 Å for d-Ge which is more than 8 times larger than $L_{\rm d-Ge}$, and 71 Å for Ge_{34} which is more than 0.5 times lager than $L_{\rm Ge_{34}}$. The convergence with smaller cell size may be attributed to the facts that the periodic boundary condition is utilized and the phonon energy at this temperature is mainly carried by the shorter wavelength phonon modes.

3.5.4. Temperature dependent thermal conductivity

Figure 10 demonstrates the calculated thermal conductivities of Ge_{34} and d-Ge calculated by the MD method in a temperature range of 200–1000 K. The $\kappa_{\rm L}$ of Ge_{34} is significantly reduced with respect to that

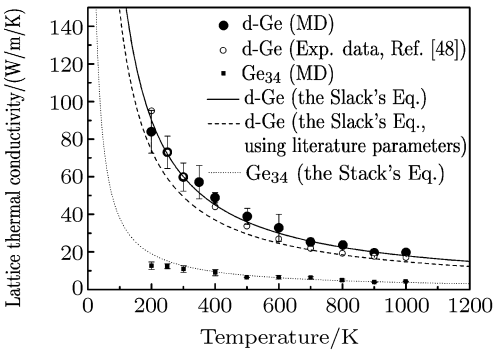


Fig. 10. Thermal conductivities of Ge_{34} and d-Ge evaluated with the MD method and the Slack's equation. The calculated thermal conductivities of d-Ge are also compared with the experimental ones.

of d-Ge in the whole temperature range. For example, $\kappa_{Ge_{34}}/\kappa_{\text{d-Ge}}$ is about 0.19 at 300 K, and 0.22 at 1000 K. For comparison, $\kappa_{Ge_{46}}/\kappa_{\text{d-Ge}}$ is found to be 0.11 at room temperature from Ref. [8].

It should be mentioned that the calculated thermal conductivities of d-Ge are in good agreement with the experimental values [48] plotted in the same figure. This is different from the previous report by Dong *et al.* By employing the EMD method and the Tersoff's potential, they found the thermal conductivity of d-Ge to be 114 W/(K·m) at 300 K, which is almost 100% larger than the experimental value or our result. The discrepancy may be partially attributed to the absence of the quantum correction in their work. We can apply the quantum correction to the result of Dong *et al.* to make a rough estimation of the 'real' thermal conductivity at room temperature ($\kappa(T_{\text{Real}} = 300\ \text{K})$). According to Eq. (8), $\kappa(T_{\text{Real}})$ is determined from the multiplication of $\kappa_{\text{MD}}(T_{\text{MD}})$ by $\text{d}T_{\text{MD}}/\text{d}T_{\text{Real}}$. From Fig. 8, one can see that $T_{\text{Real}} = 300$ K is corresponding to $T_{\text{MD}} = 331$ K and $\text{d}T_{\text{MD}}/\text{d}T_{\text{Real}}$ is equal to 0.91 at $T_{\text{Real}} = 300$ K. Due to Umklapp process, $\kappa_{\text{MD}}(T_{\text{MD}} = 331\ \text{K})$ is smaller than $\kappa_{\text{MD}}(T_{\text{MD}} = 300\ \text{K})$ which is available in Dong *et al.*'s work. If we adopt the value of $\kappa_{\text{MD}}(T_{\text{MD}} = 300\ \text{K})$ for $\kappa_{\text{MD}}(T_{\text{MD}} = 331\ \text{K})$ and take into account $\text{d}T_{\text{MD}}/\text{d}T_{\text{Real}}$, the upper limit of $\kappa(T_{\text{Real}} = 300\ \text{K})$ is found to be 104 W/K/m. Since the value is still more than 70% larger than our result, the disparity needs clarifying by making further efforts. However, we will demonstrate in the following section that our MD results are also consistent with the prediction of the Slack's equation.

3.6. Value of κ_{L} calculated by the Slack's equation

To apply the Slack's equation, the acoustic Debye temperature θ_{a} and Grüneisen parameter γ should be determined first. Bruls *et al.* proposed a simple method to estimate θ_{a} from the minimum value of the curve for Debye temperature–temperature ($\Theta - T$).[49,50] At very low temperatures, the Debye temperature is dominated by the acoustic phonon modes and it decreases with temperature increasing initially as shown in Fig. 6(b). As temperature increases, the reduction of the acoustic phonon contribution and the excitation of the optical phonon modes lead to an increase in Debye temperature. Therefore the minimum value Θ_{min} represents a good approximation for the high temperature limit of the Debye temperature associated with the acoustic phonons.[50]

The Θ_{min}, which is deduced from the specific heat data, is related to the acoustic Debye temperature in Eq. (1) by[22]

$$\theta_{\text{a,min}} = \Theta_{\text{min}} \cdot n^{-1/3}. \tag{18}$$

The Slack's equation is therefore rewritten as

$$\kappa_{\text{L}} = A\overline{M}\Theta^3_{\text{D,min}}\delta/(n^{2/3}\gamma^2 T). \tag{19}$$

In principle, γ in Eq. (19) should be contributed from all the acoustic phonon modes in the first Brillouin zone at a temperature close to the acoustic Debye temperature.[22] In the present study, γ is determined at temperature $\theta_{\text{a,min}}$ from the $\gamma - T$ curve in Fig. 7. Table 3 shows all input parameters for the Slack's equation. For d-Ge, two sets of $\theta_{\text{a,min}}$ and γ are used. One parameter set is deduced from the thermodynamic calculations in this work on the basis of Tersoff's potential. In another set, $\theta_{\text{a,min}}$ is obtained from the experimental curve in Ref. [42] (see Fig. 6(b)), and γ from *ab initio* calculation in Ref. [45] (see Fig. 7). For Ge_{34}, we use only the parameters obtained from the present work. Note that the acoustic Debye temperature of Ge_{34} is much smaller than that of d-Ge. This is understandable if we examine the phonon dispersion curves of Ge_{34} and d-Ge in Fig. 1. For Ge_{34}, the acoustic bands are 'compressed' into a low frequency region compared with those of d-Ge. This leads to a lower cutoff frequency of the acoustic phonon band which is corresponding to the lower acoustic Debye temperature of Ge_{34}.

Table 3. The parameters of the Slack's equation for Ge_{34} and d-Ge.

	$\overline{M}$/amu	δ/Å	n	$\theta_{\text{a,min}}$/K	$\gamma/\theta_{\text{a,min}}$
Ge_{34}	72.61	2.96	34	96.2	0.74
d-Ge	72.61	2.83	2	273.1	1.00
				203.6 [a]	0.70 [b]

[a]Derived from Ref. [42]. [b]Derived from Ref. [45].

The thermal conductivity curves calculated by the Slack's equation are plotted in Fig. 10 in comparison with the MD results and experimental data.[48] Based on the parameters deduced from Tersoff's potential, the κ_{L} values calculated from the Slack's equation accord pretty well with the MD results for both Ge_{34} and d-Ge above 250 K. By examining Eq. (1) and Table 3, it can be seen that reduction of κ_{L} in pristine Ge_{34} is mainly attributed to the lower acoustic Debye temperature which is caused by the complex structure.

The κ_{L} values of d-Ge predicted by the Slack's equation based on the Tersoff's potential exhibit better agreement with the experimental results than the

values calculated with the parameters reported in the literature (dash line in Fig. 10) which systematically underestimates the thermal conductivities below 500 K. In fact, Table 3 shows that the calculated values of $\theta_{\rm a,min}$ and γ for d-Ge are overestimated by the Tersoff's potential. The errors caused by the overestimations are fortunately cancelled out in Eq. (1) since $\theta_{\rm a,min}$ appears in the numerator, γ in the denominator. Nevertheless, the present work demonstrates that the combination of the Slack's equation and the empirical potential, in addition to the MD approach, provides another useful guidance for estimating the values of $\kappa_{\rm L}$ for d-Ge and Ge clathrates.

4. Conclusions

In the present study, we evaluate the lattice thermal conductivities of Ge_{34} and d-Ge with the EMD method and the Slack's equation.

The phonon propertiesare first evaluated with the lattice dynamics calculations through using the Tersoff's potential. Several thermodynamic properties including Helmholtz free energy, bulk modulus, specific heat, thermal expansion coefficient and overall Grüneisen parameter are subsequently calculated each as a function of temperature in the quasi-harmonic approximation. The parameters $\theta_{\rm a}$ and γ needed by the Slack's equation are derived from the above calculations. In the MD simulations, the thermal conductivity is calculated based on the Green–Kubo formalism in conjunction with the Tersoff's potential. Temperature scaling is included in the simulations to take into account the quantum effect.

From the simulations, three major conclusions can be drawn.

(i) The lattice thermal conductivity of d-Ge is about several times larger than that of Ge_{34} in a temperature range of 200–1000 K. The lower acoustic Debye temperature associated with the complex structure is responsible for the low lattice thermal conductivity of Ge_{34}.

(ii) The predictions of the Slack's equation which makes use of the parameters derived from the thermodynamic properties are consistent with the MD results for both Ge_{34} and d-Ge above 250 K.

(iii) The thermal conductivities of d-Ge, calculated by both methods, are comparable to the experimental results.

Acknowledgment

We would like to thank Prof. Ju Li in Ohio State University, US for kindly allowing us to modify and use the MD code developed by him and his co-workers in this work.

References

[1] San-Miguel A, Kéghélian P, Blase X, Mélinon P, Perez A, Itié J P, Polian A, Reny E, Cros C and Pouchard M 1999 *Phys. Rev. Lett.* **83** 5290
[2] Nolas G S, Cohn J L, Slack G A and Schujman S B 1998 *Appl. Phys. Lett.* **73** 178
[3] Kuznetsov V L, Kuznetsova L A, Kaliazin A E and Rowe D M 2000 *J. Appl. Phys.* **87** 7871
[4] Martin J, Nolas G S, Wang H and Yang J 2007 *J. Appl. Phys.* **102** 103719
[5] Kawaji H, Horie H, Yamanaka S and Ishikawa M 1995 *Phys. Rev. Lett.* **74** 1427
[6] Yamanaka S, Enishi E, Fukuoka H and Yasukawa M 2000 *Inorg. Chem.* **39** 56
[7] Slack G A In: Rowe D M (editor) 1995 *CRC Handbook of Thermoelectrics* (Boca Raton: CRC Press) p407
[8] Dong J, Sankey O F and Myles C W 2001 *Phys. Rev. Lett.* **86** 2361
[9] Nolas G S, Beekman M, Gryko J, Lamberton Jr G A, Tritt T M and McMillan P F 2003 *Appl. Phys. Lett.* **82** 910
[10] Li J, Porter L and Yip S 1998 *J. Nuclear Mater.* **255** 139
[11] Volz S G and Chen G 2000 *Phys. Rev.* B **61** 2651
[12] Che J, Çağın T, Deng W and Goddard III W A 2000 *J. Chem. Phys.* **113** 6888
[13] Schelling P K, Phillpot S R and Keblinski P 2002 *Phys. Rev.* B **65** 144306
[14] Tretiakov K V and Scandolo S 2004 *J. Chem. Phys.* **120** 3765
[15] Yoon Y G, Car R, Srolovitz D J and Scandolo S 2004 *Phys. Rev.* B **70** 012302
[16] Sun L and Murthy J Y 2006 *Appl. Phys. Lett.* **89** 171919
[17] Ponomareva I, Srivastava D and Menon M 2007 *Nano Lett* **7** 1155
[18] Gu X K and Cao B Y 2007 *Chin. Phys.* **16** 3777
[19] Wang H F and Chu W G 2009 *J Alloy. Compd.* **485** 488
[20] Callaway J 1959 *Phys. Rev.* **113** 1046
[21] Holland M G 1963 *Phys. Rev.* **132** 2461
[22] Morelli D T and Slack G A In: Shinde S and Goela J (editors) 2005 *High Thermal Conductivity Materials* (New York: Springer-Verlag)
[23] Fang C M and de Wijs G A 2004 *J. Phys.: Condens. Matter* **16** 3027
[24] Zhang X J, Zhang J M and Xu K W 2006 *Chin. Phys.* **15** 2108
[25] Cao L X and Wang C Y 2006 *Chin. Phys.* **15** 2092

[26] Nenghabi E N and Myles C W 2008 *Phys. Rev.* B **78** 195202
[27] Tersoff J 1989 *Phys. Rev.* B **39** 5566
[28] Gale J D 1997 *J. Chem. Soc., Faraday Trans.* **93** 629
[29] Porter L J, Li J and Yip S 1997 *J. Nuclear Mater.* **246** 53
[30] Parrinello M and Rahman A 1981 *J. Appl. Phys.* **52** 7182
[31] Allen M P and Tildesley D J 1987 *Computer Simulation of Liquids* (Oxford: Clarendon Press)
[32] Li J 2005 *J. Computer-Aided Mater. Design* **12** 141
[33] Wang H F, Chu W G, Jin H and Xiong Y F 2008 *Chem. Phys.* **344** 299
[34] Wang C Z, Chan C T and Ho K M 1990 *Phys. Rev.* B **42** 11276
[35] Dong J and Sankey O F 1999 *J. Phys.: Condens. Matter* **11** 6129
[36] Moriguchi K, Munetoh S and Shintani A 2000 *Phys. Rev.* B **62** 7138
[37] Giannozzi P, de Gironcoli S, Pavone P and Baroni S 1991 *Phys. Rev.* B **43** 7231
[38] Porter L J, Yip S, Yamaguchi M, Kaburaki H and Tang M 1997 *J. Appl. Phys.* **81** 96
[39] Porter L J, Justo J F and Yip S 1997 *J. Appl. Phys.* **82** 5378
[40] Moriguchi K, Munetoh S and Shintani A 2001 *Phys. Rev.* B **64** 195409
[41] Gibbons D F 1958 *Phys. Rev.* **112** 136
[42] Flubacher P, Leadbetter A J and Morrison J A 1959 *Philos. Mag.* **4** 273
[43] Kittel C 1996 *Introduction to Solid State Physics* (Seventh edition) (New York: John Wiley & Sons, Inc.)
[44] Sparks P W and Swenson C A 1967 *Phys. Rev.* **163** 779
[45] Ma Y and Tse J S 2007 *Solid State Commun.* **143** 161
[46] Ziman J M 1972 *Principles of the Theory of Solids* (Cambridge: Cambridge University Press)
[47] Ledbetter H M 1973 *J. Appl. Phys.* **44** 1451
[48] Glassbrenner C J and Slack G A 1964 *Phys Rev.* **134** A1058
[49] Bruls R J 2000 *The Thermal Conductivity of Magnesium Silicon Nitride $MgSiN_2$, Ceramics and Related Materials* Ph. D. Thesis, Technische Universiteit Eindhoven
[50] Bruls R, Hintzen H T and Metselaar R 2005 *J. Appl. Phys.* **98** 126101